Optimal Control of Emergency Evacuations Leveraging Equivalent Circuit Models

Joseph Moyalan * **Ricardo de Castro** * **Shuang Feng** *
Xuchang Tang ** **Xinfan Lin** ** **Scott Moura** ***

* *Dept. of Mech. Eng., University of California, Merced, USA*
** *Dept. of Mech. & Aero. Eng., University of California, Davis, USA*
*** *Dept. of Civil & Env. Eng., University of California, Berkeley, USA*

Abstract: Emergency evacuation planning is a critical task that ensures individuals' swift and safe movement from hazardous locations to designated safe zones. This paper proposes a novel *controllable equivalent circuit model* (cECM) to capture the flow of traffic in a network. The model includes switches for flow routing and additional circuit elements to represent the time lost due to recharging, which is critical for (electric) vehicles with limited driving range. We embed this cECM into a mixed-integer linear program (MILP) that determines optimal evacuation routes and recharging strategies to minimize evacuation time while considering road capacity, limited vehicle energy, and the availability of charging stations. The effectiveness of the proposed approach is demonstrated through simulations based on an evacuation case study using the Sioux Falls and Anaheim networks.

Keywords: Emergency evacuation, Equivalent circuit model, Mixed-Integer Linear Programming

1. INTRODUCTION

Emergency evacuation is a critical challenge in disaster management, where lives depend on moving people quickly and safely from danger zones. The motivation behind studying and optimizing emergency evacuation lies in minimizing casualties, improving response times, and ensuring efficient resource utilization during natural disasters. There is extensive literature that tries to solve the emergency evacuation problem by posing it as a network design problem (NDP) [Bell and Iida (1997)]. NDP formulations are difficult to scale and require meta-heuristics to solve large-scale emergency evacuation problems [Yang and H. Bell (1998)]. This work investigates the possibility of using an equivalent circuit model (ECM) to facilitate the modeling and optimization of evacuations.

ECMs allow us to apply tools from electrical engineering, such as circuit analysis laws (Ohm's and Kirchhoff's laws), and circuit elements (resistors, sources, capacitors, inductors, and switches), to gain insights into the behavior of non-electrical systems. For example, ECMs have been widely used to model heat flow, where electrical quantities such as voltage, current, and resistance are analogs of temperature, heat flux, and thermal resistance, respectively [Wunsche et al. (1997)]. Other applications that leverage ECM-based analogies include batteries and fuel cells [Amir et al. (2022)], structural and mechanical systems [Amanuel et al. (2021)], biomedical applications, and many more.

Over the last decades, ECMs have been applied to numerous transportation problems. Most ECMs build on the analogy of using current to capture the traffic flow and electrical resistance to model the cost (in time or distance) of traveling between nodes. These ECM-based models have been used to i) reduce simulation time of traffic networks, ii) predict traffic flow, and iii) identify the shortest distance/time routes. For example, [Furber (1973)] utilized electric circuits to develop an analog computer that accelerated traffic network simulations. ECMs can also be used to predict traffic flow, which is challenging to model due to the high uncertainty associated with human driving behavior. To address this, [Furber (1973); Wellin and Eisenberg (1975); Sinop et al. (2023)] build upon the hypothesis that traffic flow follows the path of least travel resistance (analogous to electrical current following the path of least electrical resistance) to predict flow in transportation networks. The results of ECM simulations can also aid in selecting the shortest distance/time paths. For instance, [Callejas-Molina et al. (2020)] applied the node-voltage method to efficiently predict traffic (current) flow between an origin and destination, then identified the shortest path by searching for branches with the highest traffic flow (current). This ECM-based route planning reduced search time compared to A* search. This concept has also attracted interest from private industry; for example, Google [Sinop et al. (2023)] leveraged electrical flow principles to determine a diverse set of routes between a source and destination, providing users with multiple options rather than a single optimal route.

This work provides two main contributions. First, we introduce a new controllable *equivalent circuit model* (cECM) that extends traffic ECMs with additional circuit

⋆ This work is supported by the California Climate Action Seed Grants of the University of California (Grant No. R02CP6996).
email: jmoyalan@ucmerced.edu

elements (switches) to regulate the flow of traffic in the network. This circuit also contains additional elements to model the time lost during re-charging, which may be particularly critical for evacuating electric vehicles with a lower driving range than conventional vehicles [Zhang and Zhang (2022); Purba et al. (2022)]. We also show how the principle of superposition [Alexander et al. (2007)] can be deployed to analyze routing problems with multiple origins and destinations.

Second contribution: We embedded the cECM into an optimization framework to generate evacuation routes that minimize the time to reach the destination while avoiding congestion on the roads and utilizing charging stations. We demonstrate that the resulting problem can be formulated as a mixed-integer linear optimization problem (MILP) [Gomory (2009)] and efficiently solved using modern numerical solvers.

2. PRELIMINARIES AND PROBLEM STATEMENT

This section introduces the notation and the problem statement of the paper.

Table 1. List of Key Parameters of the Evacuation Problem

Symbol	Description
	Transportation Parameters
$\mathcal{V}_T$	Set of vertices of the transportation network.
$\mathcal{L}_T$	Set of links of the transportation network.
d_{ij}	Distance between the nodes i and j.
T_{ij}	Free flow travelling time between the nodes i and j.
f_{ij}^{free}	Free flow capacity of the link.
k_{ij}	Density of the cars in the link.
u_{ij}^{avg}	Average speed of the cars in the link.
	Charging Paramaters
$\mathcal{L}_{ch}$	Set of links containing charging station.
$T_{ch,(ij)}$	Charging duration for station between nodes i and j.
$d_{ch,(ij)}$	Total driving range gained from the charging station.
$f_{ch,(ij)}^{max}$	Number of EVs per hour that the charger can serve.
	Evacuation Requests
$\mathcal{OD}$	Set of origin-destination pairs.
r_{od}^0	Initial driving range of vehicle.
$t_{evac,m}$	Evacuation time for the m^{th} od-pair.

2.1 Transportation network

1) Nodes: $\mathcal{V}_T = \{1, ..., N_V\}$ represents the set of vertices of the transportation network. For example, at a local level, they can capture intersections; at a regional level, they can represent a town or a city that the road reaches.
2) Links are formed by two nodes $v_i, v_j \in \mathcal{V}_T$ connected by a road; this is denoted by the link $(v_i, v_j) \in \mathcal{L}_T \subset \mathcal{V}_T \times \mathcal{V}_T$.
3)Path from node v_1 to v_l is a sequence of nodes $\mathbf{p} = [v_1, v_2, ..., v_l]$ such that $(v_k, v_{k+1}) \in \mathcal{L}_T$ for $k = 1, \ldots, l-1$, where l is total number of nodes visited along the path.
4) Weights: The distance (in miles) between two nodes is defined as $d_{ij} \in \mathbb{R}$. $\mathbf{D} = [d_{ij}]$ is a vector that contains the distances between nodes. Note: if $(i, j) \notin \mathcal{L}_T$ then $d_{i,j} = \infty$. The expected free-flow travel time (in h) between node i and j is T_{ij}. The vector $\mathbf{T} = [T_{ij}]$ captures the free-flow travel time between any two nodes. The maximum flow of vehicles (in num. vehicles/hour) that the link can support without congestion is defined as f_{ij}^{free}. The vector

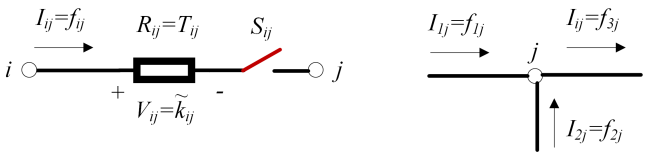

Fig. 1. ECM for a transportation link (current -> transportation flow, resistance -> travel time, voltage -> vehicle concentration).

$\mathbf{F}^{free} = [f_{ij}^{free}]$ captures the free flows between links.
5) Transportation network is denoted as a combination of the transportation graph and weights $\Theta_T = \{\mathcal{V}_T, \mathcal{L}_T, \mathbf{D}, \mathbf{F}^{free}, \mathbf{T}\}$.
Remark 1. The free-flow capacity ($\mathbf{F}^{free}$) of each link depends on vehicle density and the speed limit. Vehicle density is influenced by the number of lanes, vehicle headway, and the typical mix of vehicle types (e.g., small, medium, heavy-duty). At the same time, speed limits vary based on the surrounding area (e.g., suburbs, school zones, highways). By estimating upper bounds for both density and speed, we can derive the free-flow capacity of each link [Knoop (2017)].

2.2 Fixed Charging Network

1) Charging links: $\mathcal{L}_{ch} \subset \mathcal{L}_T$ represents a set of links containing a fixed charging station (FCS), where vehicles can recharge their batteries. We denote N_{ch} as the total number of charging links in the network.
2) Weights: The vehicles that stop in charger $(i, j) \in \mathcal{L}_{ch}$ stay stationary for a time duration $T_{ch,(i,j)}$ and receives a fixed additional range $d_{ch,(i,j)}$. This means that the EV charges at a rate of $d_{ch,(i,j)}/T_{ch,(i,j)}$ [miles/hour]. The vector $\mathbf{d}_{ch} = [d_{ch,(i,j)}]$ denotes the additional range that chargers can provide to an EV, while the vector $\mathbf{T}_{ch} = [T_{ch,(i,j)}]$ contains the expected charging time (for all chargers).
3) Re–charging decision is defined as

$$\mathbf{p}_{ch} = [(v_{ch,1}, v_{ch,2})..., (v_{ch,l_p}, v_{ch,l_p+1})]$$

such that $(v_{ch,k}, v_{ch,k+1}) \in \mathcal{L}_{ch}$. This vector indicates the charging stations the vehicle uses during the evacuation; if vehicles do not need to stop, then $\mathbf{p}_{ch} = \emptyset$.
4) We also assume that the chargers have a limit on the number of EVs they can serve per hour. We use $f_{ch,(i,j)}^{max}$ to denote the number of EVs per hour that the charger can serve. This value is dependent on the number of ports available in the charging station (n_{ports}) and the charging time allotted per vehicle (t_{ch}^{max}), and is calculated as follows:

$$f_{ch,(i,j)}^{max} = \frac{n_{ports}}{t_{ch}^{max}}$$

The vector $\mathbf{f}_{ch}^{max} = [f_{ch,(i,j)}^{max}]$ contains the limits of all chargers.
5) Charging network: The EV charging information is captured by $\Theta_{ch} = \{\mathcal{L}_{ch}, \mathbf{d}_{ch}, \mathbf{T}_{ch}, \mathbf{f}_{ch}^{max}\}$.

2.3 Evacuees, stopping and available range

1) We assume that vehicles need to evacuate from origin node $o \in \mathcal{V}_T$ to destination/shelter $d \in \mathcal{V}_T$. We assume that the destination is known in advance. We denote

$\mathcal{OD}$ the set of all possible origin-destination pairs, i.e., $m = (o,d) \in \mathcal{OD} \subset \mathcal{V}_T \times \mathcal{V}_T$. Each origin provides a flow of vehicles $f_{in,m}$.

2) Driving range: The vehicles may have different initial driving range defined as r^0_{od} for $(o,d) \in \mathcal{OD}$. To account for this variability, let us assume that we group evacuees based on their driving range $\mathbf{r}^0 = [r^0_1, r^0_2, \ldots]^T \in \mathcal{R}$. For example, r^0_1 represents vehicles with a range of at least 20 miles, r^0_2 vehicles with at least 60 miles of range, etc. These driving ranges $\mathbf{r}^0$ may be present in any of the $(o,d) \in \mathcal{OD}$.

3) Loss of driving range: Additionally, we also need to account for the loss of range along the path. This loss of range depends on the path $\mathbf{p}$ taken by the vehicles and the charging stations that are visited ($\mathbf{p}_{ch}$). This is mathematically defined as:

$$\mathbf{r}_{od} = [r_{od,1}, \ldots, r_{od,l}] \tag{1}$$

where $r_{od,1} = r^0_{od}$ is the initial driving range of the vehicle, $r_{od,k}$ is the available driving range after traveling the link k. The path is feasible if $\mathbf{r}_{od} \geq 0$.

4) Flow Constraints: When multiple origin-destination pairs use the transportation/charging network, congestion may occur. To prevent this, the overall flow of vehicles in the transportation and charging links needs to be limited:

$$\sum_{m \in \mathcal{OD}} \Phi_{ij}(\mathbf{p}_m) f_{in,m} \leq f^{free}_{ij}, \tag{2a}$$

$$\sum_{m \in \mathcal{OD}} \Phi_{ij}(\mathbf{p}_{ch,m}) f_{in,m} \leq f^{max}_{ch,(i,j)} \tag{2b}$$

where $(i,j) \in \mathcal{L}_T$ and $\Phi_{ij}(.)$ is an indicator function that return 1 if the link i,j is part of the path $\mathbf{p}_m$ and zero otherwise.

2.4 Evacuation problem with constant flows

Assumption 1. We assume that the transportation (Θ_T), charging (Θ_{ch}) and evacuee information is known. We also assume that all evacuees are leaving at the same time.

Remark 2. By stating all evacuees are leaving at the same time, we mean that the evacuation process begins almost simultaneously at the origins of all origin–destination (od) pairs, and vehicle flow starts from each origin accordingly. This does not imply that all vehicles enter the network at the same moment, but rather that the injection of vehicle flow into the network commences nearly simultaneously across all od-pairs. This assumption is consistent with macroscopic evacuation models used for evacuation planning [Purba et al. (2022); Lim et al. (2012)].

Problem 1. Given Assumption 1, find a optimal path $\mathbf{p}_{od} = [v_{1,od}, \ldots, v_{l,od}]$ connecting $(o,d) \in \mathcal{OD}$ and a re-charging strategy $\mathbf{p}_{ch,od}$ that minimizes evacuation time (t_{evac}), while complying with energy constraints ($\mathbf{r}_{od} \geq 0$) and traffic and charging flow constraints (2).

Next, we will define the emergency evacuation problem involving multiple origin-destination pairs.

Problem 2. Given Assumption 1, find optimal path $\mathbf{p}_m = [v_{1,m}, \ldots, v_{l_m,m}]$ and re-charging strategy $\mathbf{p}_{ch,m}$ by minimizing the worst evacuation time (t_{evac}) while complying with energy constraints ($\mathbf{r}_{od,m} \geq 0$) as well as traffic and charging flow constraints (2). The worst-case evacuation time is given by:

$$t_{evac} = \max(t_{evac,m}), \quad \forall\, m \in \mathcal{OD} \times \mathcal{R}.$$

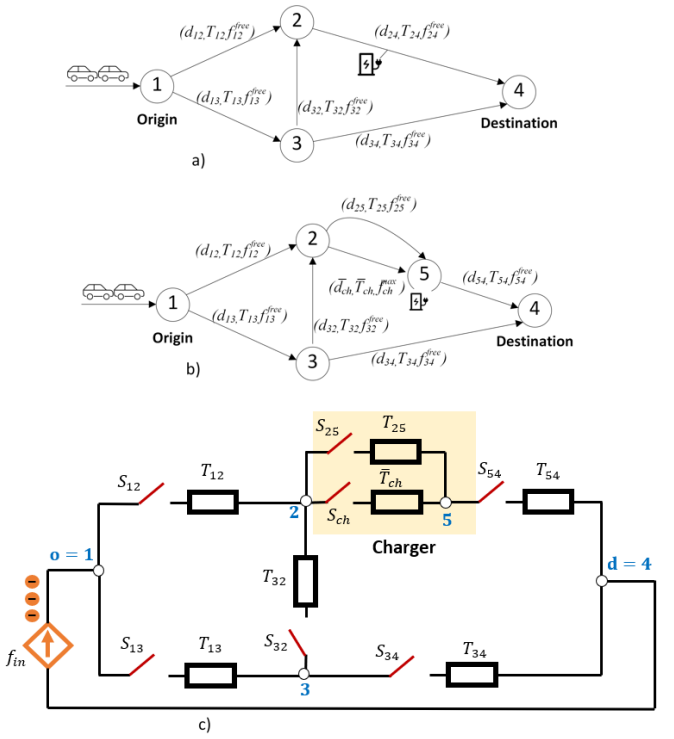

Fig. 2. (a) Transportation network graph for emergency evacuation, with node 1 as the origin and node 4 as the destination. (b) Modified transportation graph including an artificial node 5, representing a charging station. The two links between nodes 2 and 5 model the decision to either utilize the charging station or bypass it. (c) Controllable ECM model is proposed in this study, where resistors represent travel time and electrical current emulates traffic flow, with charged particles symbolizing vehicles. The binary switch variables S_{ij}, obtained through optimization, determine the links selected for evacuation routing.

where $t_{evac,m}$ represents the minimum evacuation time along the path $\mathbf{p}_m$.

3. EVACUATION PLANNING WITH ECM

This section introduces ECM to help facilitate the solution of optimal evacuation problems.

3.1 Transportation Network Laws

Recall the fundamental (macroscopic) relationship [Knoop (2017)] in a traffic link:

$$f_{ij} = k_{ij} u^{avg}_{ij} \tag{3}$$

where k_{ij} [in vehicles/miles] is the density of cars in the link $i \to j$, f_{ij} [in vehicles/hour] is the flow, and u^{avg}_{ij} [in miles/hour] is the average speed in the link. The previous relationship can also be rewritten as

$$f_{ij} = (k_{ij} d_{ij}) \left(u^{avg}_{ij}/d_{ij}\right) = \tilde{k}_{ij}/T_{ij} \tag{4}$$

The term $\tilde{k}_{ij} = k_{ij} d_{ij}$ denotes the total number of vehicles on the link $i \to j$ at any given time while $T_{ij} = \left(u^{avg}_{ij}/d_{ij}\right)^{-1}$ represents the expected travel time for the link. Consider the node j with three links and

corresponding flows f_{1j}, f_{2j}, f_{j3} (Fig. 1). Links f_{1j} and f_{2j} are "incoming" links, while link f_{j3} is an "outgoing link". They must fulfill the flow balance constraint:

$$f_{1j} + f_{2j} = f_{3,j} \tag{5}$$

Note that all the above relations assume steady-state operation of the traffic.

3.2 Controllable Equivalent Circuit Model (cECM)

The fundamental traffic relationship (4)-(5) has the same structure as Ohm's law[1] and Kirchhoff's current law (KCL), where,

- Traffic node j is equivalent to an electric node j.
- Traffic link $i \to j$ is equivalent to an electric branch $i \to j$.
- Vehicle flow f_{ij} equivalent to current I_{ij}.
- The number of vehicles $\tilde{k}_{ij} = k_{ij}d_{ij}$ is equivalent to voltage drop between node i and j (V_{ij}).
- Travel time T_{ij} is equivalent to a resistance R_{ij}.

Table 2. Analogy between traffic network and electrical circuits

Traffic network	Electrical circuit
traffic flow (f_{ij})	current (I_{ij})
Number of vehicles ($\tilde{k}_{ij}$)	Voltage diff. (V_{ij})
Travel time (T_{ij})	Resistor (R_{ij})
Fundamental macroscopic relation	Ohm's Law
$f_{ij} = \tilde{k}_{ij}/T_{ij}$	$I_{ij} = V_{ij}/R_{ij}$
Flow conservation	Kirchhoff's current law (KCL)
$f_{1j} + f_{2j} = f_{3j}$	$I_{1j} + I_{2j} = I_{3j}$
Route selection	Electrical switches

Fig. 1 depicts the equivalent circuit representing the flow between node i and node j, which mimics (4)-(5). The equivalent circuit also contains a switch $S_{ij} \in \{0, 1\}$, which allows us to enable/disable the flow of current (traffic flow) between links.

Fig. 2 depicts an example of a transportation network for emergency evacuation with 4 links and one charger (located between nodes 2 and 4). To facilitate the derivation of the ECM, we introduce the artificial node 5, which is connected to both nodes 2 (through two links) and 4, as shown in Fig. 2b. The two links defined through parameters $(d_{25}, T_{25}, f_{25}^{free})$ and $(\bar{d}_{ch}, \bar{T}_{ch}, f_{ch}^{max})$ represents the choice of either bypassing the charging station or utilizing it respectively, while going from node 2 to node 4 through node 5. Here, $\bar{d}_{ch} = d_{ch} - d_{25}$ and $\bar{T}_{ch} = T_{ch} + T_{25}$. Similarly, we can generalize this for any number of charging stations through vectors $\bar{\mathbf{d}}_{ch} = [\bar{d}_{ch,(i,j)}]$ and $\bar{\mathbf{T}}_{ch} = [\bar{T}_{ch,(i,j)}]$. Fig. 2c depicts the corresponding ECM with 5 nodes and 7 links. Node $o = 1$ is the origin node. It is connected with a current source that provides a continuous flow of vehicles (for the evacuation). The current can then "flow" in different branches (equivalents of road links). The current is allowed to flow in the branch (i, j) if the switch S_{ij} is enabled. The switch indicates whether the path is used for the evacuation or not. For the two links between node 2 and 5, the choice of utilizing the charging station depends on the switch S_{ch}.

[1] Recall $I = V/R$, where V is the voltage, R is the resistance, and I is the current.

Assumption 2. We assume that all the vehicles of an origin-destination pair travel together without splitting into multiple routes. Also, all vehicles travel at a constant free-flow speed in the transportation network.

Decision variables: In what follows, we will treat the following variables as decision variables:

- $\mathbf{S} = [S_{12}, S_{13}, ...]^T \in \mathbb{B}^{N_L}$ is a set of boolean variables that indicate if traffic is allowed to flow in a given non-charging link/branch. Here, $\mathbb{B} = \{0, 1\}$ is a Boolean set and N_L represents links without the charging stations.
- $\mathbf{S}^{ch} = [S_{12}^{ch}, S_{13}^{ch}, ...]^T \in \mathbb{B}^{N_{ch}}$ is a set of boolean variables that indicate if traffic is allowed to flow in a given charging link/branch.

Transportation flow matrix: We will apply KCL to the nodes of the example depicted in Fig. 2c, where the current is replaced with vehicle flow multiplied by the link switches. For example, applying KCL at node 1, we get

$$f_{12} + f_{13} = f_{in} \tag{6}$$

However, utilizing Assumption 2, we know that

$$f_{12} = f_{in}S_{12},\ f_{13} = f_{in}S_{13} \tag{7}$$

Therefore, utilizing (6) and (7), we get

$$f_{in}(S_{12} + S_{13}) = f_{in} \tag{8}$$

Similarly, applying KCL to all nodes of Fig. 2c allows us to obtain the following relations:

$$\text{(node 1)}: \quad f_{in}(S_{12} + S_{13}) = f_{in} \tag{9}$$
$$\text{(node 2)}: \quad f_{in}(S_{12} + S_{32} - S_{25} - S_{ch}) = 0 \tag{10}$$
$$\text{(node 3)}: \quad f_{in}(S_{13} - S_{32} - S_{34}) = 0 \tag{11}$$
$$\text{(node 4)}: \quad f_{in}(S_{54} + S_{34}) = f_{in} \tag{12}$$
$$\text{(node 5)}: \quad f_{in}(S_{ch} + S_{25} - S_{54}) = 0 \tag{13}$$

This can be compactly rearranged into a matrix form:

$$\mathbf{A}_{KCL}\mathbf{S} + \mathbf{A}_{KCL}^{ch}\mathbf{S}^{ch} = \mathbf{B}_{KCL} \tag{14}$$

where $\mathbf{A}_{KCL} \in \mathbb{R}^{N_V \times N_L}$, $\mathbf{A}_{KCL}^{ch} \in \mathbb{R}^{N_V \times N_{ch}}$, $\mathbf{B}_{KCL} \in \mathbb{R}^{N_V \times 1}$ are matrices that depend on the configuration of the circuit/transportation network.

Travel time: We can approximate the total travel time in the network by summing up the resistances that are used in the circuit. This means

$$t_{evac}(\mathbf{S}, \mathbf{S}^{ch}) = \mathbf{T}^T\mathbf{S} + \bar{\mathbf{T}}_{ch}^T\mathbf{S}^{ch} \tag{15}$$

Driving range: In Fig. 2, we start in node o with a driving range r^0. We then drive d_{12}, stop in the charger to gain $\bar{d}_{ch}$, and finally drive d_{54}, reaching the destination node. The driving range (r_{end}) at the end of the journey is given by:

$$r_{end} = r^0 - d_{12} + \bar{d}_{ch} - d_{54} \tag{16}$$

If $r_{end} > 0$, then the route is feasible; otherwise, the driver will need to stop in more places or find a different route. This can be written compactly in the vector form for all the links as follows:

$$r^0 - \mathbf{D}^T\mathbf{S} + \bar{\mathbf{d}}_{ch}^T\mathbf{S}^{ch} \geq 0 \tag{17}$$

which needs to be positive for the path to be physically feasible for the vehicle. We assume that all the vehicles considered in this paper have enough r_0 to reach at least the nearest FCS location.

Based on this ECM for the transportation network, we can compute the flows in each branch to minimize the (upper-

bound) evacuation time in the network. This leads to the following simplified optimization problem:

$$\min_{\mathbf{S},\mathbf{S}^{ch}} t_{evac}(\mathbf{S},\mathbf{S}^{ch}) \tag{18}$$

$$\text{s.t.} \quad (14),(17) \tag{19}$$

Remark 3. All the cost terms and equations are linear. The above problem is an Integer linear programming (ILP) that can be tackled using modern solvers such as [Gurobi Optimization, LLC (2024)].

3.3 Multiple origins and destinations

We will extend the previous example to the case with multiple origins and destinations. Let us consider $m = ((o,d),r^0) \in \mathcal{OD}\times\mathcal{R}$ as an admissible od-pair. We denote $f_{in,m}$ as the input flow injected at the origin of m.

We propose the use of the principle of superposition to analyze the problem with multiple od pairs. Let us consider the od-pair $m = ((o,d),r^0)$, while disabling the other od pairs ($f_{in,l} = 0$, for $l \neq m$). We analyze the contribution of each current source, one at a time:

$$\mathbf{A}_{KCL}\mathbf{S}_m + \mathbf{A}^{ch}_{KCL}\mathbf{S}^{ch}_m = \mathbf{B}_{KCL,m} \tag{20}$$

where $\mathbf{S}_m$, $\mathbf{S}^{ch}_m$ are the switches for non-charging and charging routes for vehicles linked with the od pair m. $\mathbf{B}_{KCL,m}$ is a column vector obtained from injecting a flow $f_{in,m}$ in the node associated with origin o for $m \in \mathcal{OD}\times\mathcal{R}$.

The overall flows in each transpiration link can be evaluated by adding the contribution of each od-pair: $\sum_m f_{in,m}$. This total flow needs to fulfill the free-flow constraint of the non-charging link given by

$$0 \leq \sum_m f_{in,m}\mathbf{S}_m \leq \mathbf{F}^{free}_T \tag{21}$$

and the total charging capacity of the charging station

$$0 \leq \sum_m f_{in,m}\mathbf{S}^{ch}_m \leq \mathbf{f}^{max}_{ch}. \tag{22}$$

We can now compute the optimal paths for each od-pair using the following formulation :

$$\min_{\mathbf{s}_m,\mathbf{S}^{ch}_m,\gamma,t_{evac,m}} \gamma \tag{23}$$

$$\text{s.t.} \quad (20)-(22) \tag{24}$$

$$\mathbf{T}^T\mathbf{S}_m + \bar{\mathbf{T}}^T_{ch}\mathbf{S}^{ch}_m = t_{evac,m},\ t_{evac,m} \leq \gamma \tag{25}$$

$$r^0_m - \mathbf{D}^T\mathbf{S}_m + \bar{\mathbf{d}}^T_{ch}\mathbf{S}^{ch}_m \geq 0,\ m \in \mathcal{OD}\times\mathcal{R} \tag{26}$$

where $t_{evac,m}$ is the expected evacuation time of the od-pair m and γ is a slack variable.

This problem aims to minimize the worst-case evacuation time among all the od pairs. The first set of constraints evaluates each od-pair's flows and evacuation times. The last set of equations relies on the superposition principle to evaluate the overall flow in each link and ensure that it does not exceed the link's free-flow limit. The input flows $f_{in,m}$ represent the input parameters that can be varied.

Remark 4. The above problem is an MILP.

Up to now, we have been focusing on minimizing the worst-case evacuation time among all the evacuees ($J^{max} = t_{evac}$). In what follows, we will consider two additional cost functions: *average evacuation time* (J^{avg}) and *worst-case variation in evacuation time* (J^{Δ}):

$$J^{avg} = \frac{1}{M}\sum_m t_{evac,m}, \quad J^{\Delta} = \max_m |t_{evac,m} - J^{avg}| \tag{27}$$

where M is the total number of od-pairs in the set $\mathcal{OD}\times\mathcal{R}$. The cost function for the evacuation problem can be posed as the weighted sum of these three cost terms, leading to the following general optimal evacuation planning:

$$\mathbb{P}: \min w_{max}J^{max} + w_{avg}\theta J^{avg} + w_{\Delta}(1-\theta)J^{\Delta}$$
$$\text{s.t.} \quad (24)-(26)$$

where $w_{max}, w_{avg}, w_{\Delta} \geq 0$ are user-defined weights, and $\theta \in [0,1]$ is a trade-off parameter that allows the designer to penalize (worst-case) variance. This last term is motivated by fairness in the route allocation, since some evacuees may be reluctant to follow routes with longer evacuation times. This work considers three types of planning strategies that penalize:

- $\mathbb{P}^{max}$: max. evacuation time among all OD pairs ($w_{max} = 1, w_{avg} = w_{\Delta} = \theta = 0$)
- $\mathbb{P}^{avg}$: average evacuation time ($w_{avg} = 1, w_{max} = w_{\Delta} = \theta = 0$)
- $\mathbb{P}^{avg+\Delta}$: average and max. variation in evacuation time ($w_{avg} = w_{\Delta} = 1, w_{max} = 0$)

4. SIMULATION RESULTS

To validate the evacuation plans, we considered the transportation networks of Sioux Falls [Ukkusuri and Yushimito (2009); Purba et al. (2022)] and Anaheim [Network (2025)]. The locations of the fixed charging stations (FCS) for both networks were obtained from [PlugShare (2025)]. We will be utilizing only the location of FCS with DC fast charging capability that can provide a charging rate (d_{ch}/T_{ch}) of 200 miles/hour corresponding to the DC fast charging speed (to facilitate fast evacuation). We perform all the simulations using Python 3.19 on a Dell computer with 32 GB of Random Access Memory (RAM) and an Intel(R) i9-13900HX processor (2.20 GHz). We use Gurobi 12.0 as our optimization toolbox.

4.1 Sioux Falls

The Sioux Falls transportation network has 24 nodes and 38 edges (see Fig. 3). This section discusses the evacuation problem, containing six evacuation od-pairs. We use the modified map of Sioux Falls, which is based on the region's geography, but with an extended range seven times the original topography [Tang et al. (2024)]. The edges of the network have a free flow capacity (f^{free}_{ij}) ranging between 1800 and 2200 vehicles/hour [Ukkusuri and Yushimito (2009)]. We assume that the initial state of charge (SOC) of vehicles participating in the emergency evacuation for the Sioux Falls network corresponds to a driving range (r_0) of 50 miles (i.e., 20% of full battery capacity). This assumption is conservative and ensures a realistic lower-bound estimate for available energy during evacuation. We also assume that the input flow (f_{in}) at all six od-pairs is equal to 50 vehicles/hour. This is consistent with the EV population of Sioux Falls for the year 2024, which observes close to only 300 electric vehicles [Survey (2024)].

Fig. 3 showcases the optimal route (shown in blue) for one of the od-pairs of the Sioux Falls case, obtained by solving $\mathbb{P}^{max}$. The black nodes represent network nodes.

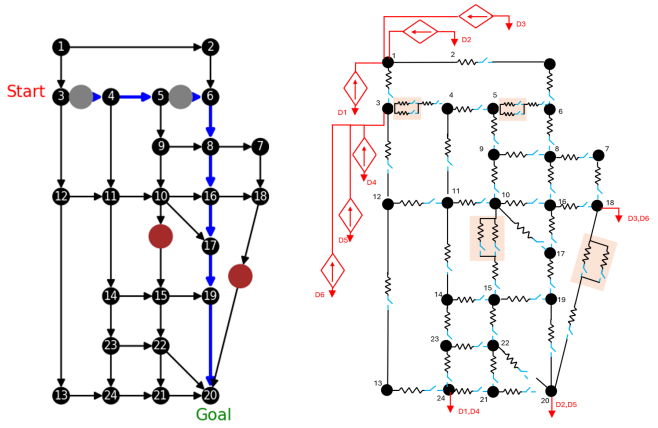

Fig. 3. (Left) The optimal route (shown in blue) for the od-pair, $m = (3, 20)$ and $\mathbb{P}^{max}$. The black nodes represent network nodes. The grey/red nodes represent FCS. The red (grey) nodes indicate the FCS is unused (used) for that route. (Right) ECM of the evacuation problem.

The grey/red nodes represent FCS. The red (grey) nodes indicate the FCS is unused (used) for that route.

Fig. 4 provides a sensitivity study of the impact of the initial range (r_0) in the cost functions of the three evacuation strategies ($\mathbb{P}^{max}$, $\mathbb{P}^{avg}$ and $\mathbb{P}^{avg+\Delta}$). When comparing $\mathbb{P}^{avg}$ and $\mathbb{P}^{max}$, one can observe that $\mathbb{P}^{avg}$ reduces the average evacuation time by around 4% for $r_0 = 50$ miles. Closer inspection for $r_0 = 50$ miles reveals that 3 od-pairs require more than 1.7 hrs to evacuate with $\mathbb{P}^{max}$. On the other hand, only 2 od-pairs [2] exceed 1.7 hrs with $\mathbb{P}^{avg}$. Overall, $\mathbb{P}^{avg}$ reduces the evacuation time for most of the od-pairs when compared to $\mathbb{P}^{max}$. The results obtained with $\mathbb{P}^{avg+\Delta}$ show that this evacuation strategy can reduce the spread in the evacuation, especially for $r_0 \geq 60$ miles.

Fig. 5 shows the impact of θ on the cost functions. One can observe that when $\theta \to 0$, the worst-case variation in evacuation time shrinks, which "equalizes" the time needed to reach the destination among all evacuees. The price to pay for this equalization is an increase in evacuation time: when $\theta = 1$, we need (on average) 1.45 hrs to evacuate, while $\theta = 0$ requires 1.78 hrs average evacuation time (a 22.7% increase).

Fig. 6 shows the normalized flow values of different edges for the Sioux Falls network for various values of input flow (f_{in}). We can observe that as f_{in} increases, the flow values approach the (free-flow) capacity of the link. For high input flows, the optimizer splits traffic among more links (e.g., links 26-32) to prevent violating the free-flow constraints. These results illustrate the "traffic-aware" evacuation planning offered by $\mathbb{P}$.

Finally, Fig. 7 shows normalized flow values ($f_{ij}/f^{max}_{ch,(ij)}$) of FCS for the Sioux Falls network for various values of initial range (r_0). We observe that as r_0 decreases, more and more FCS are being utilized to overcome the deficiency in the traveling range of the vehicles.

Figures 8 and 9 compare ECM-based evacuation planning with shortest-path routing using the $A^\star$ algorithm. The

[2] two od-pairs are overlapping at 1.31 hrs

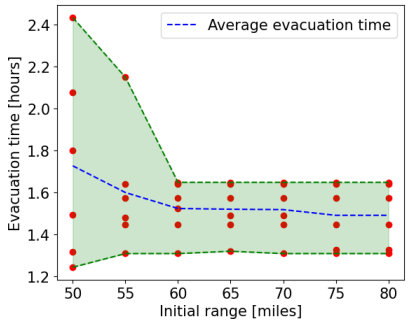

(a) Minimizing worst-case evacuation time ($\mathbb{P}^{max}$)

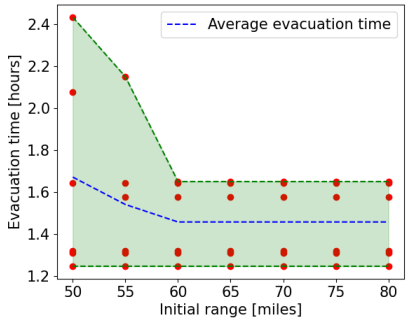

(b) Minimizing average evacuation time ($\mathbb{P}^{avg}$)

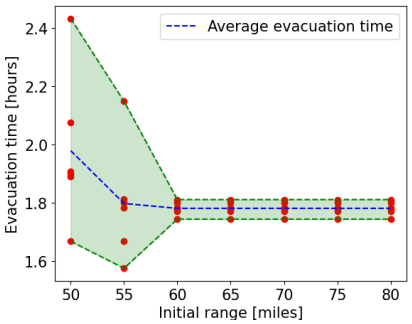

(c) Minimizing worst-case variation in evacuation time ($\mathbb{P}^{avg+\Delta}$)

Fig. 4. Comparison of different performance indices for the Sioux Falls case. The red dots in the plot represent the evacuation times for the six od-pairs.

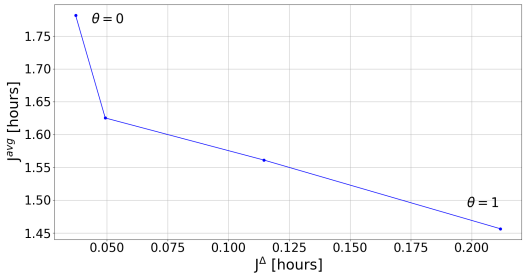

Fig. 5. Values of the performance indexes for different range of θ ($r_0 = 80$ miles) obtained with $\mathbb{P}^{avg+\Delta}$.

A* algorithm determines the shortest path between the origin and the destination. However, if the vehicle lacks sufficient r_0 to reach the destination, the algorithm will first identify the shortest path to the nearest FCS. Once

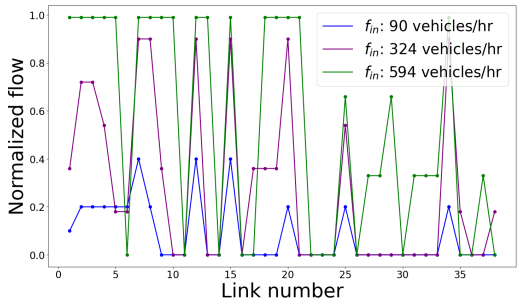

Fig. 6. The normalized flow values (f_{ij}/f_{ij}^{free}) of different edges for the Sioux Falls network for various values of input flow (f_{in}).

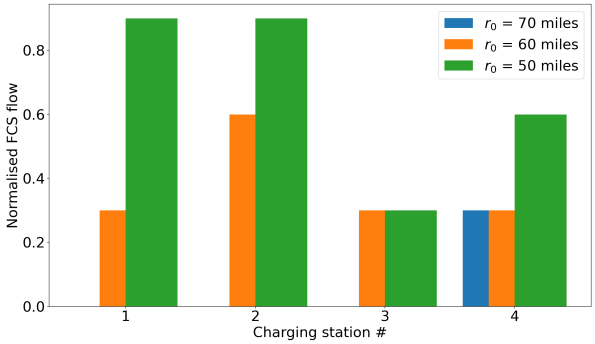

Fig. 7. The normalized flow values ($f_{ij}/f_{ch,(i,j)}^{max}$) of fixed charging stations (FCS) for the Sioux Falls network for various values of initial range (r_0).

the vehicle reaches the FCS, the algorithm will then find the shortest path from the FCS to the final destination. The scenario considers a traffic incident that reduces the free-flow capacity of the link between nodes 3 and 4 from 1800 to 200 vehicles/hour due to lane blockages. Figure 8 presents the normalized flow across each link. The $A^\star$ algorithm results in congestion on the affected link, as it forms part of the shortest route for all six od-pairs. In contrast, ECM-MILP generates evacuation routes that respect the reduced capacity of each link.

Figure 9 shows the normalized flow rate at each of the four FCS in the Sioux Falls map. The normalized flow rate is defined as the ratio of the vehicle arrival rate to the total service rate of the FCS. Under the $A^\star$ routing strategy, 4 out of 6 od-pairs require charging to reach their destinations, and all are routed to the same FCS located on the link between nodes 3 and 4. Consequently, the normalized flow rate at this FCS exceeds 1, indicating that the vehicle arrival rate surpasses its service capacity, leading to queuing delays. In contrast, the ECM-MILP approach distributes traffic more evenly across the network by utilizing all available FCSs. This ensures that the normalized flow rate at each station remains below 1, effectively eliminating queuing and reducing overall evacuation time. These results highlight the advantage of ECM-based optimization in enabling more efficient and traffic-aware evacuation planning.

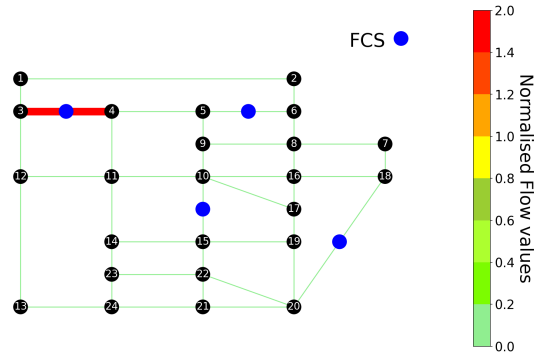

(a) $A^\star$ algorithm

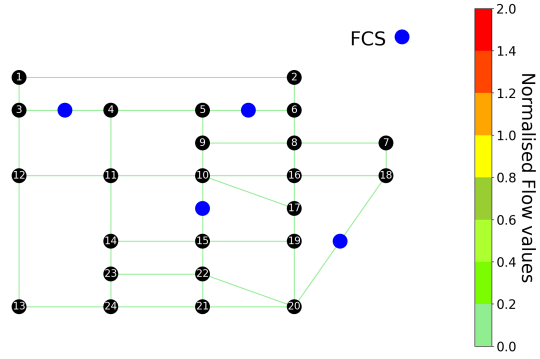

(b) ECM-MILP

Fig. 8. Comparison of normalized flow values (f_{ij}/f_{ij}^{free}) of different edges for the Sioux Falls network between $A^\star$ algorithm and ECM-MILP. Here, $f_{ij}^{free} = 200$ vehicles/hour for the link connecting nodes 3 and 4 due to a traffic incident blocking most of the lanes of this road section.

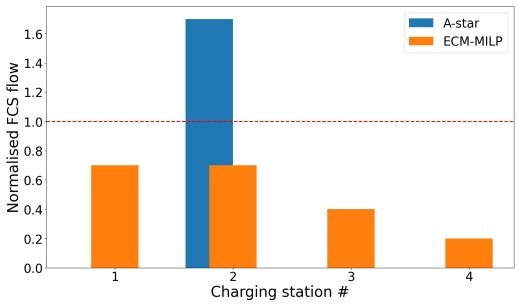

Fig. 9. Comparison of the normalized flow rate at each of the four FCS used in the Sioux Falls map.

4.2 Anaheim Network

The Anaheim transportation network has 416 nodes and 914 edges (See Fig. 10). This section discusses the evacuation problem, containing four evacuation od-pairs. The edges of the network have the free flow capacity (f_{ij}^{free}) ranging between 1800 to 12600 vehicles/hour [Network (2025)]. We assume that the SOC of vehicles participating in the emergency evacuation for this network corresponds to a driving range (r_0) of 6-50 miles (i.e., $2\% - 20\%$ of full battery capacity). We also assume that the input flow (f_{in}) at all four od-pairs is equal to 1500 vehicles/hour. This is consistent with the EV population of Orange County,

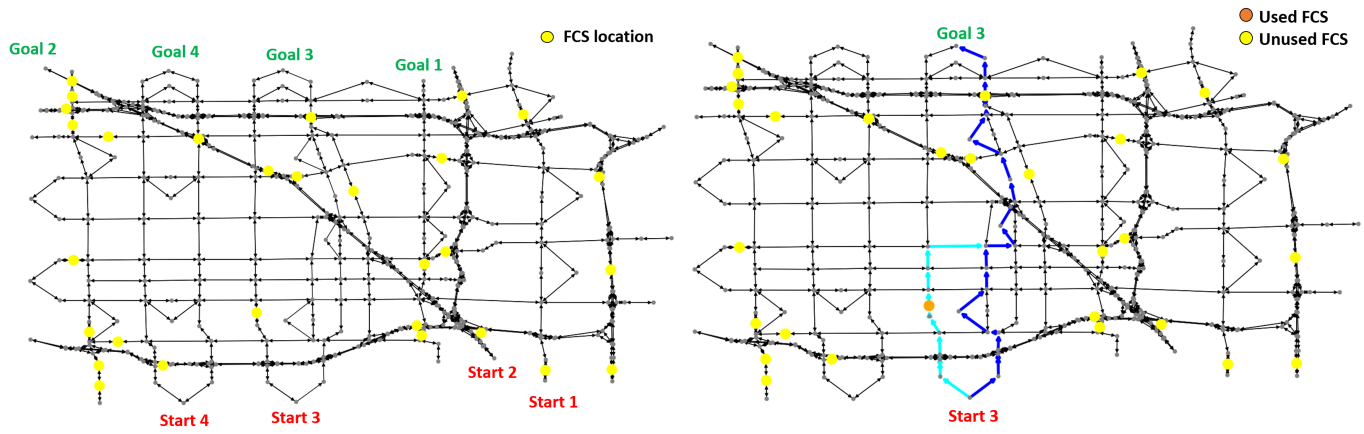

(a) (b)

Fig. 10. (a) Anaheim network with all the start and goal nodes as well as the location of all fast charging FCSs. (b) Optimal route (shown in blue) for the od-pair, $m = (18, 10)$ and $\mathbb{P}^{avg}$. The vehicles for this od-pair are divided into two groups based on whether their r_0 is sufficient. Vehicles with sufficient range proceed directly to the goal via the shortest travel-time route (shown in navy blue). In contrast, vehicles with insufficient range take a detour (shown in sky blue) to the nearest FCS, where they recharge to gain the required range before eventually merging with the main route taken by the sufficient group.

California, where the Anaheim network is located, which was estimated at approximately 134,000 electric vehicles in 2024 [Survey (2025)]. Since Anaheim constitutes roughly 1/10 population of Orange County, the same can be assumed for the EV population. Fig. 10a showcases all the start and goal nodes as well as the location of all fast charging FCSs. Fig. 10b showcases the optimal route (shown in blue) for one of the od-pairs of the Anaheim network, obtained by solving $\mathbb{P}^{avg}$. The yellow (orange) nodes indicate the FCS is unused (used) for that route. In this case, some vehicles have an initial range of $r_0 = 6$ miles, which is insufficient to reach the destination. As a result, the vehicles for this od-pair are divided into two groups based on whether their r_0 is sufficient. Vehicles with sufficient range proceed directly to the goal via the shortest travel-time route (shown in navy blue). In contrast, vehicles with insufficient range take a detour (shown in sky blue) to the nearest FCS, where they recharge to gain the required range before eventually merging with the main route taken by the sufficient group.

A comparison of the computation time with respect to the number of od-pairs can be found in Table 3 for the Sioux Falls and Anaheim networks. Therefore, in terms of scalability, the MILP framework for ECM-based optimization can generate solutions within 1.42 hours for networks comprising 416 nodes and 914 links for up to 15 od-pairs. When considering implementation at the county or state level, the solver's computational time will primarily depend on the size of the network, specifically the number of nodes and links. One approach to mitigate this challenge is to simplify the network. For instance, the Anaheim case study discussed earlier can be significantly reduced by aggregating certain road segments and assuming conservative estimates for road capacity. Such simplifications can significantly reduce the solver's computational burden.

Table 3. Computation time comparison

# **OD-pairs**	**Sioux Falls** 24 nodes, 38 links	**Anaheim** 416 nodes, 914 links
2	0.32 seconds	30.75 seconds
4	0.34 seconds	55.184 seconds
8	0.56 seconds	1.85 minutes
10	1.2 seconds	2.01 minutes
15	2.2 seconds	1.42 hours
20	3.7 seconds	$>$ 5 hours

4.3 Tool for evacuation planners

The results presented in this paper can be used for planning evacuations before the occurrence of a natural disaster, especially in communities that are prone to wildfires, floods, and hurricanes that usually trigger evacuations. Some of the ways in which ECM-based optimization can be used for planning an emergency scenario are as follows:

(1) By utilizing ECM-MILP, we can generate evacuation routes and analyze traffic congestion under various vehicle flow scenarios (Fig. 6). This allows us to identify bottlenecks both along road segments (Fig. 8a) and at different FCS locations (Fig. 9). Early identification of these issues will enable us to modify the network proactively, helping to prevent disruptions during an actual emergency, such as deploying mobile charging stations at high traffic routes.

(2) By simulating various evacuation scenarios (Fig. 4), first responders can identify which od-pairs require the most time to evacuate under different conditions, such as SOC, population density, and the pace of disaster progression. This insight enables emergency personnel and traffic authorities to better coordinate vehicle flows, prioritize critical areas, and ultimately reduce total evacuation time.

(3) Urban planners can use such tools to pre-position mobile chargers or design resilient charging networks, while smart city developers can embed these strategies into real-time traffic and energy management systems.

5. CONCLUSION AND FUTUREWORK

We presented a novel approach to formulating the emergency evacuation problem using a new controllable equivalent circuit model (cECM). We have shown that the optimization of the cECM for the evacuation problem can be posed as a mixed-integer linear program (MILP) to provide routing and re-charging strategies that minimize the overall evacuation time, while complying with flow and energy constraints. Numerical simulation results with the use cases inspired by Sioux Falls and Anaheim networks demonstrated the effectiveness of the proposed approach under different evacuation scenarios.

Future extensions of this work will explore the integration of the cECM with mobile chargers and real-time evacuation planning. We also intend to relax the assumption that all evacuees depart simultaneously by incorporating time-varying current sources, allowing us to model varying traffic flows at the origin. Additionally, the assumption that all vehicles travel at the same free-flow speed will be refined by introducing the Bureau of Public Roads (BPR) function [Mtoi and Moses (2014); Maerivoet and De Moor (2005)], which captures the nonlinear relationship between travel time and traffic congestion. Further research will consider stochastic behavior and partial compliance among evacuees, with validation performed using high-fidelity traffic simulators.

REFERENCES

Alexander, C.K., Sadiku, M.N., and Sadiku, M. (2007). *Fundamentals of electric circuits*. McGraw-Hill Higher Education Boston, MA, USA.

Amanuel, T., Ghirmay, A., Ghebremeskel, H., Ghebrehiwet, R., and Bahlibi, W. (2021). Design of vibration frequency method with fine-tuned factor for fault detection of three phase induction motor. *Journal of Innovative Image Processing (JIIP)*.

Amir, S., Gulzar, M., Tarar, M.O., Naqvi, I.H., Zaffar, N.A., and Pecht, M.G. (2022). Dynamic equivalent circuit model to estimate state-of-health of lithium-ion batteries. *Ieee Access*, 10.

Bell, M.G. and Iida, Y. (1997). *Transportation network analysis*. Wiley Online Library.

Callejas-Molina, R.A., Diaz-Carmona, J., Vazquez-Leal, H., Mayorga-Cruz, D., and Lopez-Leal, R. (2020). Exploring a novel electrical-modeling-based route planning for vehicle guidance. *Mathematical Problems in Engineering*, 2020(1), 4348964.

Furber, C.P. (1973). *Electrical circuit simulation of traffic flow*. The University of Arizona.

Gomory, R.E. (2009). Outline of an algorithm for integer solutions to linear programs and an algorithm for the mixed integer problem. In *50 Years of integer programming 1958-2008: From the early years to the State-of-the-Art*, 77–103. Springer.

Gurobi Optimization, LLC (2024). Gurobi Optimizer Reference Manual. URL `https://www.gurobi.com`.

Knoop, V.L. (2017). Introduction to traffic flow theory: An introduction with exercises. *Delft University of Technology: Delft, The Netherlands*.

Lim, G.J., Zangeneh, S., Baharnemati, M.R., and Assavapokee, T. (2012). A capacitated network flow optimization approach for short notice evacuation planning. *European Journal of Operational Research*, 223(1), 234–245.

Maerivoet, S. and De Moor, B. (2005). Transportation planning and traffic flow models. *arXiv preprint physics/0507127*.

Mtoi, E.T. and Moses, R. (2014). Calibration and evaluation of link congestion functions: applying intrinsic sensitivity of link speed as a practical consideration to heterogeneous facility types within urban network. *Journal of Transportation Technologies*, 2014.

Network, A. (2025). Transportation networks for research core team. Technical report, Transportation Networks for Research. URL `https://github.com/bstabler/TransportationNetworks`.

PlugShare (2025). Plugshare data tool. Technical report, plugshare.com. URL `https://company.plugshare.com/`.

Purba, D.S.D., Kontou, E., and Vogiatzis, C. (2022). Evacuation route planning for alternative fuel vehicles. *Transportation research part C: emerging technologies*, 143, 103837.

Sinop, A.K., Fawcett, L., Gollapudi, S., and Kollias, K. (2023). Robust routing using electrical flows. *ACM Transactions on Spatial Algorithms and Systems*, 9(4), 1–25.

Survey, A. (2025). Zev and infrastructure stats data. Technical report, California Energy Commission. URL `https://www.energy.ca.gov/files/zev-and-infrastructure-stats-data`.

Survey, S.F. (2024). Sioux falls electric vehicle readiness study. Technical report, City of Sioux Falls. URL `https://www.siouxfalls.gov/government/sustainability/projects-events/ev-study`.

Tang, X., Lin, X., Feng, S., Markolf, S., de Castro, R., Gan, Q., and Moura, S. (2024). Enhancing large-scale evacuations of electric vehicles through integration of mobile charging stations. In *2024 IEEE 27th International Conference on Intelligent Transportation Systems (ITSC)*, 1494–1501. IEEE.

Ukkusuri, S.V. and Yushimito, W.F. (2009). A methodology to assess the criticality of highway transportation networks. *Journal of Transportation Security*, 2(1), 29–46.

Wellin, J. and Eisenberg, L. (1975). Simulation of traffic flow using electrical network parameters. *Journal of the Franklin Institute*.

Wunsche, S., Clauß, C., Schwarz, P., and Winkler, F. (1997). Electro-thermal circuit simulation using simulator coupling. *IEEE Transactions on very large scale integration (VLSI) systems*.

Yang, H. and H. Bell, M.G. (1998). Models and algorithms for road network design: a review and some new developments. *Transport Reviews*, 18(3), 257–278.

Zhang, J. and Zhang, X. (2022). A multi-trip electric bus routing model considering equity during short-notice evacuations. *Transportation Research Part D: Transport and Environment*.

